ISBN: 978-3-95450-248-6 ISSN: 2673-5490 doi: 10.18429/JACoW-IPAC2025-WEPM067

INTRODUCING AN OPEN-SOURCE 3D TIME-DOMAIN ELECTROMAGNETIC WAKEFIELD SOLVER FOR BEAM-COUPLING IMPEDANCE SIMULATIONS

E. de la Fuente*[1], L. Giacomel, G. Iadarola, G. Rumolo, C. Zannini, CERN, Geneva, Switzerland
M. Cotelo, Instituto de Fusion Nuclear Guillermo Velarde (IFN-GV), Madrid, Spain
[1] also at Universidad Politecnica de Madrid (UPM), Madrid, Spain

Abstract

The determination of electromagnetic wakefields and their impact on accelerator performance is a longstanding challenge in accelerator physics. These wakefields, induced by the interaction between a charged particle beam and the surrounding vacuum chamber structures, significantly affect beam stability and power dissipation. Accurate characterization of these effects via beam-coupling impedance is crucial for predicting and mitigating performance limitations. While analytical methods are sufficient for simple geometries, realistic accelerator components require full-wave, three-dimensional numerical solutions of Maxwell's equations. In alignment with CERN's Open Science initiative, this contribution introduces an open-source 3D electromagnetic time-domain solver specifically designed for computing wake potentials and impedance in arbitrary geometries. The solver's numerical implementation, optimized for CUDA-enabled GPUs, is presented and validated through benchmarks against established commercial codes. By fostering a collaborative framework, this solver aspires to address emerging challenges in accelerator design.

INTRODUCTION

The evaluation of beam-coupling impedance and wakefields are critical in the design and operation of particle accelerators. As charged particle beams traverse accelerator structures, interactions with geometric discontinuities and material inhomogeneities generate electromagnetic (EM) fields—known as wakefields—these can degrade beam stability, cause beam-induced heating, and limit machine performance [1]. The frequency-domain counterpart of these interactions is the beam-coupling impedance, an intrinsic property of each component used to quantify wakefield effects.

Analytical methods provide accurate impedance predictions for simplified structures such as resistive walls [2, 3], RF cavities [4, 5], and transitions such as tapers or steps [6–8]. However, for realistic accelerator components with complex geometries, the full three-dimensional solution of Maxwell's equations [9] is required. Equations (1a)–(1d) represent them in integral form, describing the evolution of the electric field **E**, magnetic flux density **B**, electric displacement field **D**, and magnetic field intensity **H**, in the presence of a current density **J** and charge density ρ. The constitutive relations in Eq. (1e) relate these fields through the material properties: permittivity ε, permeability μ, and conductivity σ, with **v** denoting the velocity of moving charges.

$$\oint_{\partial A} \mathbf{E} \cdot \mathrm{d}\mathbf{s} = -\iint_{A} \frac{\partial \mathbf{B}}{\partial t} \cdot \mathrm{d}\mathbf{A} \tag{1a}$$

$$\oint_{\partial A} \mathbf{H} \cdot \mathrm{d}\mathbf{s} = \iint_{A} \left(\frac{\partial \mathbf{D}}{\partial t} + \mathbf{J} \right) \cdot \mathrm{d}\mathbf{A} \tag{1b}$$

$$\oiint_{\partial V} \mathbf{B} \cdot \mathrm{d}\mathbf{A} = 0 \tag{1c}$$

$$\oiint_{\partial V} \mathbf{D} \cdot \mathrm{d}\mathbf{A} = \iiint_{V} \rho \, \mathrm{d}V \tag{1d}$$

$$\mathbf{D} = \varepsilon \mathbf{E}, \quad \mathbf{B} = \mu \mathbf{H}, \quad \mathbf{J} = \sigma \mathbf{E} + \rho \mathbf{v} \tag{1e}$$

Maxwell's equations can be solved numerically in either frequency or time domain. In the frequency domain, for lossless and source-free structures, the problem reduces to an eigenmode formulation, as used in CST Eigenmode, HFSS, or ACE3P's Omega3P. In contrast, time-domain solvers offer full-wave impedance characterization by directly computing Eqs. (1a)–(1d). Commercial solvers such as CST Wakefield, GDFiDL, and closed-source ECHO3D [10] and PBCI [11] report to use the Finite Integration Technique (FIT) [12], while ACE3P's T3P employs the Finite Element Method (FEM) [13].

Several 3D open-source solvers implement full-wave time-domain methods, such as Meep [14] and WarpX [15], both based on the Finite-Difference Time-Domain (FDTD) method [16], and EMcLaW [17], which uses a Finite-Volume Time-Domain (FVTD) Godunov scheme. However, these tools lack key features needed for beam-coupling impedance calculations—such as native CAD geometry support, advanced material modeling, or wakefield-tailored post-processing.

In alignment with CERN's Open Science initiative, the `Wakis` project started as a post-processing tool to compute impedance from pre-computed EM fields [18]. The tool was later coupled to open-source solvers like WarpX, achieving successful cavity benchmarks below cutoff. These initial implementations exposed limitations in geometry handling, material support, and code modularity. This motivated the development of `Wakis` as a full open-source, Python-based, 3D time-domain EM solver tailored for wakefield and impedance simulations in arbitrary geometries.

* elena.de.la.fuente.garcia@cern.ch

ISBN: 978-3-95450-248-6 ISSN: 2673-5490 doi: 10.18429/JACoW-IPAC2025-WEPM067

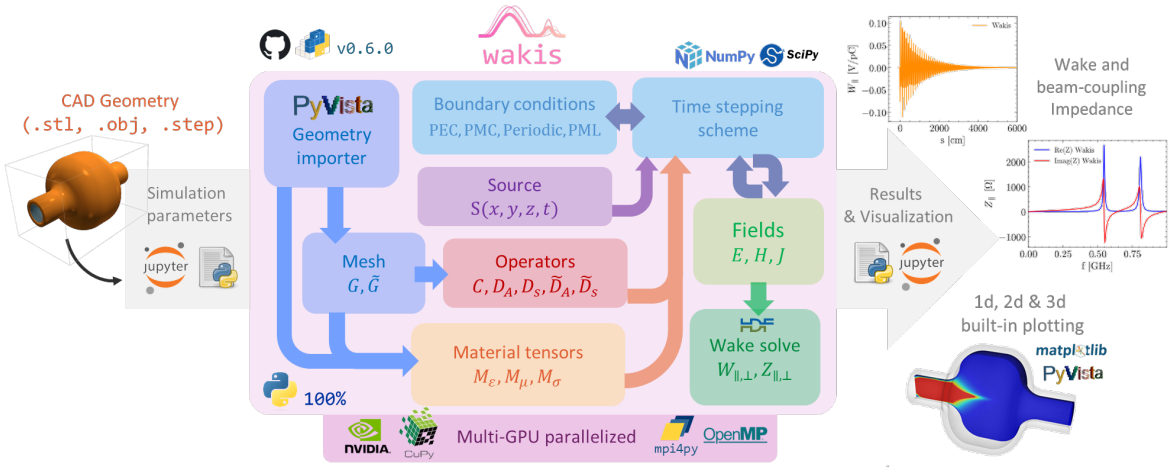

Figure 1: `Wakis` (v0.6.0) code architecture diagram.

IMPLEMENTATION

Following established practices in commercial solvers, `Wakis` adopts the Finite Integration Technique (FIT) for the numerical solution of Maxwell's equations, as described in [19–21]. In this formulation (1a)–(1d) are discretized on a Cartesian grid of $N_{cells} = N_x N_y N_z$ computational cells using a staggered Yee lattice [16]. Assuming charge-free and source-free initial conditions, the divergence equations (1c) and (1d) are inherently satisfied and need not be solved explicitly. The resulting Maxwell Grid Equations describe the time evolution of the fields:

$$\mathbf{C}\mathbf{D}_s\,\mathbf{e} = -\mathbf{D}_A\,\frac{\partial(\mathbf{M}_\mu \mathbf{h})}{\partial t} \tag{2a}$$

$$\widetilde{\mathbf{C}}\widetilde{\mathbf{D}}_s\,\mathbf{h} = \widetilde{\mathbf{D}}_A\left(\frac{\partial(\mathbf{M}_\varepsilon \mathbf{e})}{\partial t} + \mathbf{M}_\sigma \mathbf{e} + \mathbf{j}_{\mathrm{src}}\right) \tag{2b}$$

Here, $\mathbf{e}$ and $\mathbf{h}$ are the electric and magnetic field vectors for each cell, stored in memory as `numpy` $\{1 \times 3N_{cells}\}$ arrays in lexicographic order, and encapsulated within a `Field` class with methods for optimized operations, inspection, and matrix transformation. The discrete curl operators $\mathbf{C}$ and $\widetilde{\mathbf{C}} = \mathbf{C}^T$ are sparse $\{3N_{cells} \times 3N_{cells}\}$ matrices with bands of $+1$ and -1, stored as CSR matrices using `scipy.sparse`. $\mathbf{D}_s$, $\widetilde{\mathbf{D}}_s$, $\mathbf{D}_A$, and $\widetilde{\mathbf{D}}_A$ are diagonal matrices representing cell edge lengths and face areas in the primal and dual ($\sim$) grids. The permittivity, permeability, and conductivity tensors are encoded in the sparse matrices $\mathbf{M}_\varepsilon$, $\mathbf{M}_\mu$, and $\mathbf{M}_\sigma$, respectively, supporting anisotropy. The term $\mathbf{j}_{\mathrm{src}}$ represents the external current source density.

To advance fields in time, `Wakis` uses the Leapfrog scheme, a second-order accurate explicit method:

$$\mathbf{h}^{n+1} = \mathbf{h}^n - \Delta t\,\widetilde{\mathbf{D}}_s\,\mathbf{M}_\mu^{-1}\,\mathbf{D}_A^{-1}\,\mathbf{C}\,\mathbf{e}^{n+0.5} \tag{3a}$$

$$\begin{aligned}\mathbf{e}^{n+1.5} = \mathbf{e}^{n+0.5} &+ \Delta t\,\mathbf{D}_s\,\widetilde{\mathbf{M}}_\varepsilon^{-1}\,\widetilde{\mathbf{D}}_A^{-1}\,\widetilde{\mathbf{C}}\,\mathbf{h}^n \\ &- \widetilde{\mathbf{M}}_\varepsilon^{-1}\,\mathbf{j}_{\mathrm{src}}^n - \widetilde{\mathbf{M}}_\varepsilon^{-1}\,\widetilde{\mathbf{M}}_\sigma\,\mathbf{e}^{n+0.5}\end{aligned} \tag{3b}$$

These equations are evaluated at every time step Δt, where the timestep is constrained by the Courant-Friedrichs-Lewy (CFL) condition and material relaxation times. Most matrix products are pre-computed and cached to minimize memory usage and computational overhead, achieving ≈ 20 million computational cells in less than 8 GBs of cached memory.

The solver accepts arbitrary initial conditions for E, H, or J. Time-dependent sources are handled via user-defined callbacks before each timestep. Additionally, several predefined sources types (e.g., dipole, plane wave, laser pulse) are available and have been helpful to verify the numerical implementation. For beam-coupling impedance studies, a rigid Gaussian beam is modeled as a longitudinal line source [22]:

$$\mathbf{J_z}(x_{src}, y_{src}, \mathbf{z}) = \frac{q\beta c}{\sqrt{2\pi}\sigma_z}\,e^{-\frac{(\mathbf{s}-s_0)^2}{2\sigma_z^2}} \tag{4}$$

where $\mathbf{s} = \mathbf{z} - \beta c t$ is the beam-frame coordinate and $s_0 = z_{\min} - \beta c t_{\mathrm{inj}}$ denotes the bunch center, with t_{inj} the beam injection time. This formulation supports both ultra-relativistic and low-β regimes.

To terminate fields at the simulation domain boundaries, `Wakis` includes several boundary condition (BC) options: perfect electric (PEC) and magnetic (PMC) conductors are enforced by zeroing relevant rows or columns, respectively, in the curl matrix $\mathbf{C}$, while periodic BCs are implemented through ghost cell synchronization. Recently, absorbing boundaries using perfectly matched layers (PMLs) [23] were added, allowing simulation of accelerator devices above cut-off frequencies. The PML layers achieve adiabatic reflection [24] using spatially ramped conductivity profiles in the last n_{PML} cells.

`Wakis` supports CAD geometry importing and meshing via `PyVista` [25]. 3D models in `.STL`, `.OBJ`, and `.STEP` formats are meshed and mapped onto the rectangular computational grid, though an improved smart meshing algorithm is envisioned for future releases. The input material properties in each x, y, z direction (ε_r, μ_r, σ) are assigned to the

ISBN: 978-3-95450-248-6 ISSN: 2673-5490 doi: 10.18429/JACoW-IPAC2025-WEPM067

occupied cells via a first-order -MEEP inspired- sub-pixel smoothing and the material matrices $\mathbf{M}_\varepsilon$, $\mathbf{M}_\mu$, and $\mathbf{M}_\sigma$ are built accordingly.

GPU acceleration is available through `CuPy` and `cupyx`, providing seamless replacement of `NumPy/SciPy` operations when GPU computation is enabled. Multi-GPU and multi-CPU parallelization is supported via OpenMPI using `mpi4py`, with load-balanced domain decomposition performed in the longitudinal direction.

`Wakis` is fully open-source and available on GitHub [26] strictly following the Github Community Standards. The code is documented with `Sphinx` and includes continuous integration/deployment (CI/CD) practices, with nightly end-to-end tests performed with GitHub Actions, and automated packaging of releases to `PyPI`. A wide range of examples scripts and Jupyter notebooks are included in the repository. Figure 1 offers a glimpse of the modular software architecture and computation flow.

SIMULATION BENCHMARKS

`Wakis` has been continuously benchmarked throughout its development. The computed electromagnetic fields have been successfully validated against textbook analytical solutions, including the propagation of a Gaussian wave-packet through dielectric interfaces or the resonant excitation of a PEC box at the TEM_{010} frequency. A systematic benchmarking campaign against CST Studio's Wakefield Solver has also been conducted, covering structures such as smooth pipes, geometric transitions, and resonant cavities with varying material conductivities, across both ultra-relativistic and low-β regimes. These benchmarks are publicly available in a dedicated GitHub repository, which will be expanded with increasingly complex case studies.

Figure 2 shows results for CST's example suite accelerator cavity, with diameter $\varnothing = 46$ cm and length $L = 35$ cm, simulated for different cavity shell conductivities. The beam parameters were set to $\sigma_z = 0.02$ m and $q = 1$ nC, exciting frequencies up to 5 GHz above the pipe cutoff at ~ 2.2 GHz. The computed wake potentials show excellent agreement in both short- and long-range behavior, particularly in the decay trends associated with conductivity changes. The impedance spectra reveal the cavity's fundamental and harmonic modes, which decrease in amplitude until cutoff (shaded area), where modes in propagation are absorbed by the PML BCs. The inset plot highlights the main resonant peak, where minor discrepancies could be attributed to the lossy metal approximation in the CST simulation.

To ensure a fair comparison, both solvers used computational meshes of 11.4 million cells, corresponding to approximately 20 cells per shortest wavelength. The CST simulation, executed on a 16-core Intel Broadwell CPU using YZ and XZ symmetries, required 5 hours, 20 minutes, and 11 seconds to simulate a wakefield of 100 m length. In contrast, `Wakis`, running on a single NVIDIA Titan V GPU, completed the simulation in 58 minutes and 16 seconds, achieving a $5\times$ speedup under these conditions.

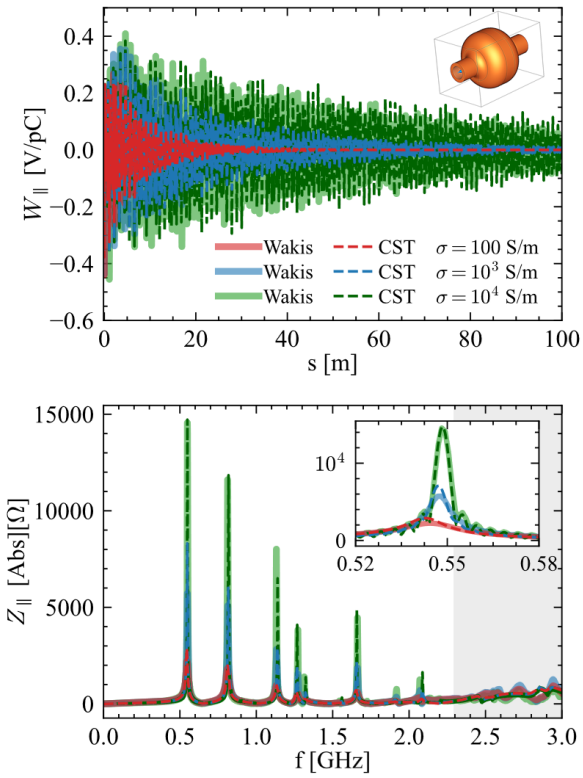

Figure 2: Comparison of wake potential (top) and longitudinal impedance magnitude (bottom) between `Wakis` and CST® Wakefield solver for a lossy cavity.

CONCLUSIONS

Developed as the first fully open-source initiative, `Wakis` is a three-dimensional electromagnetic time-domain solver designed to address beam-coupling impedance challenges in complex accelerator geometries. Based on the Finite Integration Technique (FIT) and discretized on a Cartesian Yee lattice, it solves Maxwell's equations with flexible material modeling, CAD importing, and a wide range of boundary conditions, including adiabatic PMLs. Hosted on GitHub, the source code is entirely in Python, leveraging optimized open-source libraries such as `NumPy`, `SciPy`, and `PyVista`. The solver supports GPU acceleration with `CuPy` and multi-CPU/GPU execution via `mpi4py`. Deployed to `PyPI`, its continuous integration and best open-science practices ensure robustness, transparency, and community accessibility.

Benchmark comparisons against CST Studio's Wakefield Solver demonstrate its accuracy and competitiveness. `Wakis` has already seen positive reception, with envisioned applications for muon collider, and FCC-ee impedance model development. Future releases will expand its capabilities with surface impedance models, dispersive materials, and advanced meshing. The project aims to serve as a stepping-stone for collaborative development, enabling the community to collectively address present and future challenges in impedance studies.

ISBN: 978-3-95450-248-6 ISSN: 2673-5490 doi: 10.18429/JACoW-IPAC2025-WEPM067

REFERENCES

[1] E. Metral, G. Rumolo, and W. Herr, "Impedance and Collective Effects," in *Particle Physics Reference Library, Volume 3: Accelerators and Colliders*. 2020, pp. 105–181, doi:10.1007/978-3-030-34245-6_4

[2] K. Yokoya, "Resistive wall impedance of beam pipes of general cross section," *Part. Accel.*, vol. 41, pp. 221–248, 1993, https://cds.cern.ch/record/248630

[3] M. Migliorati, L. Palumbo, C. Zannini, N. Biancacci, and V. G. Vaccaro, "Resistive wall impedance in elliptical multilayer vacuum chambers," *Phys. Rev. Accel. Beams*, vol. 22, no. 12, p. 121 001, 2019, doi:10.1103/PhysRevAccelBeams.22.121001

[4] A. Hofmann and B. W. Zotter, "Analytic models for the broad band impedance," 1990, https://cds.cern.ch/record/196446

[5] E. Jensen, "RF Cavity Design," CERN, Tech. Rep. CERN-2014-009.405, 2014, Comments: 25 pages, contribution to the CAS - CERN Accelerator School: Advanced Accelerator Physics Course, Trondheim, Norway, 18-29 Aug 2013, doi:10.5170/CERN-2014-009.405

[6] K. Yokoya, "Impedance of slowly tapered structures," CERN, Tech. Rep. CERN-SL-90-88-AP, 1990, https://cds.cern.ch/record/210347

[7] G. Stupakov, "Low frequency impedance of tapered transitions with arbitrary cross sections," *Phys. Rev. Spec. Top. Accel. Beams*, vol. 10, no. 9, 2007, doi:10.1103/PhysRevSTAB.10.094401

[8] L. Palumbo, V. G. Vaccaro, and M. Zobov, "Wake fields and impedance," Tech. Rep. LNF-94-041-P, 1994, pp. 331–390, doi:10.5170/CERN-1995-006.331

[9] J. C. Maxwell, "VIII. A dynamical theory of the electromagnetic field," *Philos. Trans. R. Soc. Lond.*, vol. 155, pp. 459–512, 1865, Publisher: Royal Society, doi:10.1098/rstl.1865.0008

[10] I. Zagorodnov. "ECHO4D." (), https://echo4d.de

[11] T. Lau, E. Gjonaj, R. Maekinen, and T. Weiland, "Computation of Resistive Wall Wakefields with the PBCI Code," in *Proc. EPAC'08*, Genoa, Italy, 2008, paper TUPP095, pp. 1753–1755, https://jacow.org/e08/papers/TUPP095.pdf

[12] T. Weiland, "Finite Integration Method and Discrete Electromagnetism," en, *Comput. Electromagn.*, pp. 183–198, 2003, doi:10.1007/978-3-642-55745-3_12

[13] A. Grudiev *et al.*, "ACE3P Computations of Wakefield Coupling in the CLIC Two-beam Accelerator," in *Proc. LINAC'10*, Tsukuba, Japan, Sep. 2010, paper MOP025, pp. 106–108, https://jacow.org/LINAC2010/papers/MOP025.pdf

[14] A. F. Oskooi, D. Roundy, M. Ibanescu, P. Bermel, J. D. Joannopoulos, and S. G. Johnson, "Meep: A flexible free-software package for electromagnetic simulations by the fdtd method," *Comput. Phys. Commun.*, vol. 181, no. 3, pp. 687–702, 2010, doi:10.1016/j.cpc.2009.11.008

[15] L. Fedeli *et al.*, "Pushing the Frontier in the Design of Laser-Based Electron Accelerators with Groundbreaking Mesh-Refined Particle-In-Cell Simulations on Exascale-Class Supercomputers," in *SC22: International Conference for High Performance Computing, Networking, Storage and Analysis*, 2022, pp. 1–12, doi:10.1109/SC41404.2022.00008

[16] K. Yee, "Numerical solution of initial boundary value problems involving maxwell's equations in isotropic media," *IEEE Trans. Antennas Propag.*, vol. 14, no. 3, pp. 302–307, 1966, doi:10.1109/TAP.1966.1138693

[17] J. A. Moreno, E. Oliva, and P. Velarde, "EMcLAW: An unsplit Godunov method for Maxwell's equations including polarization, metals, divergence control and AMR," *Comput. Phys. Commun.*, vol. 260, p. 107 268, 2021, doi:10.1016/j.cpc.2020.107268

[18] E. de la Fuente, C. Zannini, G. Iadarola, and L. Giacomel, "A generalized tool to compute wake potential and impedance from electromagnetic time domain simulations," in *Proc. IPAC'23*, Venice, Italy, 2023, pp. 3522–3525, doi:10.18429/JACoW-IPAC2023-WEPL170

[19] T. Weiland and R. Wanzenberg, "Wake fields and impedances," *Lect. Notes Phys.*, vol. 400, pp. 39–79, 1992, doi:10.1007/3-540-55250-2_26

[20] L. Hänichen, "Numerical calculation of beam Coupling Impedances in Synchrotron Accelerators," en, Ph.D. Thesis, Technische Universität Darmstadt, 2016, https://tuprints.ulb.tu-darmstadt.de/5367/

[21] K. Klopfer, "Computation of Complex Eigenmodes for Resonators Filled With Gyrotropic Materials," ger, Ph.D. Thesis, Technische Universität Darmstadt, 2014, https://tuprints.ulb.tu-darmstadt.de/id/eprint/4210

[22] M. C. Balk, R. Schuhmann, and T. Weiland, "Open boundaries for particle beams within fit-simulations," *Nucl. Instrum. Methods Phys. Res. A*, vol. 558, no. 1, pp. 54–57, 2006, doi:10.1016/j.nima.2005.11.076

[23] J.-P. Berenger, "A perfectly matched layer for the absorption of electromagnetic waves," *J. Comput. Phys.*, vol. 114, no. 2, pp. 185–200, 1994, doi:10.1006/jcph.1994.1159

[24] A. F. Oskooi, L. Zhang, Y. Avniel, and S. G. Johnson, "The failure of perfectly matched layers, and towards their redemption by adiabatic absorbers," EN, *Opt. Express*, vol. 16, no. 15, pp. 11 376–11 392, 2008, Publisher: Optica Publishing Group, doi:10.1364/OE.16.011376

[25] C. B. Sullivan and A. A. Kaszynski, "PyVista: 3D plotting and mesh analysis through a streamlined interface for the Visualization Toolkit (VTK)," en, *J. Open Source Softw.*, vol. 4, no. 37, p. 1450, 2019, doi:10.21105/joss.01450

[26] E. de la Fuente Garcia. "Wakis." available at https://github.com/ImpedanCEI/wakis. (), https://github.com/ImpedanCEI/wakis